International Journal of Research
Special Issue in UGC Approved Journal
Available at https://edupediapublications.org/journals
e-ISSN: 2348-6848
p-ISSN: 2348-795X
Volume 04 Issue 11
September 2017

PV Cell fed Step-up Resonant Converter for Induction Motor Drive Application

VENKATA KIRAN KATRAGADDA
[1]PG Scholar,
Dept of EEE, BVCITS, Batlapalem,
Amalapuram, AP, India.

A BHIMA RAJU
[2]Assistant Professor,
Dept of EEE, BVCITS, Batlapalem,
Amalapuram, AP, India.

Abstract- In the hybrid micro grid, processes of multiple dc-ac dc or ac-dc-ac conversions are reduced in an individual ac or dc grid. The hybrid grid consists of both ac and dc networks connected together by multi directional converters. In this micro grid network, it is especially difficult to support the critical load without incessant power supply. The generated power can be extracted under varying wind speed, solar irradiation level and can be stored in batteries at low power demands. In this paper, a hybrid AC-DC micro grid with solar energy, energy storage, and a pulse load is proposed. This micro grid can be viewed as a PEV parking garage power system or a ship's power system that utilizes sustainable energy and is influenced by a pulse load. The battery banks inject or absorb energy on the DC bus to regulate the DC side voltage. The frequency and voltage of the AC side are regulated by a bidirectional AC-DC inverter. The power flow control of these devices serves to increase the system's stability and robustness. The system is simulated in MATLAB/SIMULINK.

Key Words: Renewable energy, resonant converter, soft switching, voltage step-up, voltage stress.

I. INTRODUCTION

In general, manufacturers provide 5 second and ½ an hour surge figures which give an indication of how much power is supplied by the inverter. Solar inverters require a high efficiency rating. Since use of solar cells remains relatively costly, it is paramount to adopt high efficiency inverter to optimize the performance of solar energy system. High reliability helps keep maintenance cost low. Since most solar power stations are built in rural areas without any monitoring manpower, it requires that inverters have competent circuit structure, strict selection of components and protective functions such as internal short circuit protection, overheating protection and overcharge protection. Wider tolerance to DC input current plays an important role, since the terminal voltage varies depending on the load and sunlight [1-4]. Though energy storage batteries are significant in providing consistent power supply, variation in voltage increases as the battery's remaining capacity and internal resistance condition changes especially when the battery is ageing, widening its terminal voltage variation range. In mid-to-large capacity solar energy systems, inverters' power output should be in the form of sine waves which attain less distortion in energy transmission. Many solar energy power stations are equipped with gadgets that require higher quality of electricity grid which, when connected to the solar systems, requires sine waves to avoid electric harmonic pollution from the public power supply.[5] How Inverters Work: There are three major functions an inverter provides to ensure the operation of a solar system One of the most efficient and promising way to solve this problem is the use of pumping and water treatment systems supplied by photovoltaic (PV) solar energy. Such systems aren't new, and are already used for more than three decades [6-8].

But until recently the majority of the available commercial converters are based on an intermediate storage system performed with the use of batteries or DC motors to drive the water pump. The batteries allow the system to always operate at its rated power even in temporary conditions of low solar radiation [9-10]. This facilitates the coupling of the electric dynamics of the solar panel and the motor used for pumping. Generally, batteries used in this type of system have a low life span, only two years on average, which is extremely low compared to useful life of 15 years of a photovoltaic module. Also, they make the cost of installation and maintenance of such systems substantially high. Furthermore, the lack of batteries replacement is responsible for total failure of such systems in isolated areas this type of system normally uses low-voltage DC motors, thus avoiding a boost stage between the PV module and the motor [11].

Unfortunately, DC motors have low efficiency and high maintenance cost and is not suitable. For such applications the use of a three phase induction motor, due to its high degree of robustness, low cost, higher efficiency and lower maintenance cost compared to other types of motors. These requirements make necessary use of a converter with features high efficiency; low cost; autonomous operation; robustness and high life span [12-13].

II. CONVERTER STRUCTURE AND OPERATION PRINCIPLE

The proposed resonant step-up converter is shown in Fig. 1. The converter is composed of an FB switch network,

International Journal of Research
Special Issue in UGC Approved Journal
Available at https://edupediapublications.org/journals
e-ISSN: 2348-6848
p-ISSN: 2348-795X
Volume 04 Issue 11
September 2017

which comprises Q_1 through Q_4, an LC parallel resonant tank, a voltage doubler rectifier, and two input blocking diodes, D_{b1} and D_{b2}.

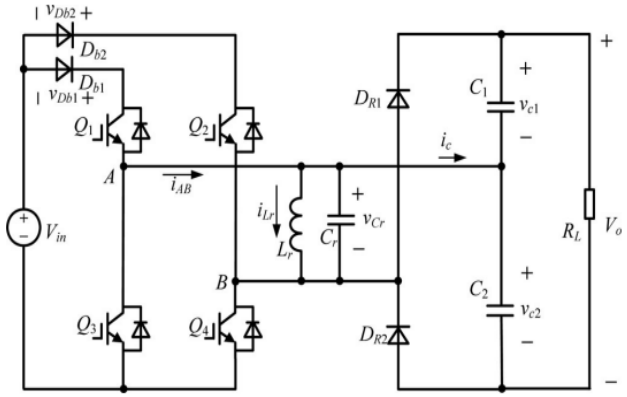

Fig. 1. Topology of the proposed resonant step-up converter.

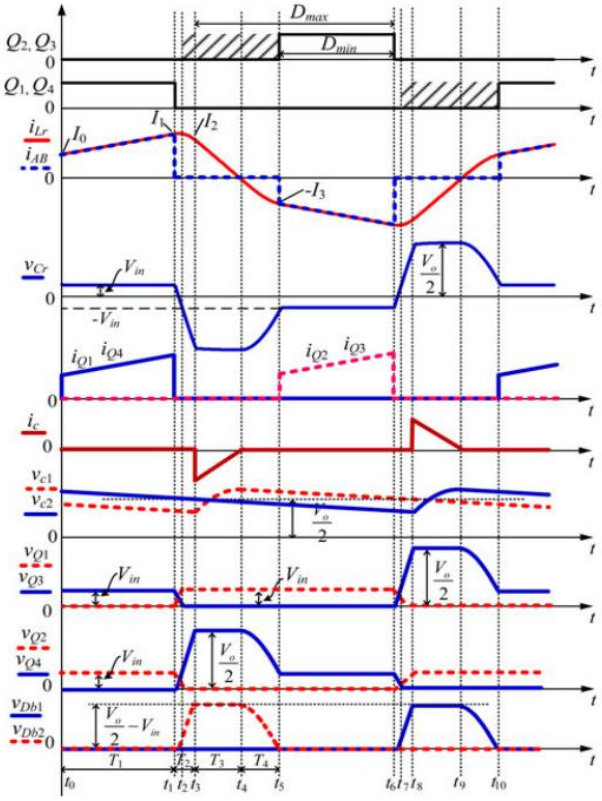

Fig. 2. Operating waveforms of the proposed converter.

The steady-state operating waveforms are shown in Fig. 2 and detailed operation modes of the proposed converter are shown in Fig. 3. For the proposed converter, Q_2 and Q_3 are tuned on and off simultaneously; Q_1 and Q_4 are tuned on and off simultaneously. In order to simplify the analysis of the converter, the following assumptions are made:

1) all switches, diodes, inductor, and capacitor are ideal components;

2) Output filter capacitors C_1 and C_2 are equal and large enough so that the output voltage V_O is considered constant in a switching period Ts.

A. Mode 1 [t_0, t_1] [See Fig. 3(a)]

During this mode, Q_1 and Q_4 are turned on resulting in the positive input voltage V_{in} across the LC parallel resonant tank, i.e., $v_{Lr} = v_{C\,r} = V_{in}$. The converter operates similar to a conventional boost converter and the resonant inductor L_r acts as the boost inductor with the current through it increasing linearly from I_0. The load is powered by C_1 and C_2. At t_1, the resonant inductor current i_{Lr} reaches I_1

$$I_1 = I_0 + \frac{V_{\text{in}} T_1}{L_r} \quad (1)$$

Where T_1 is the time interval of t_0 to t_1.

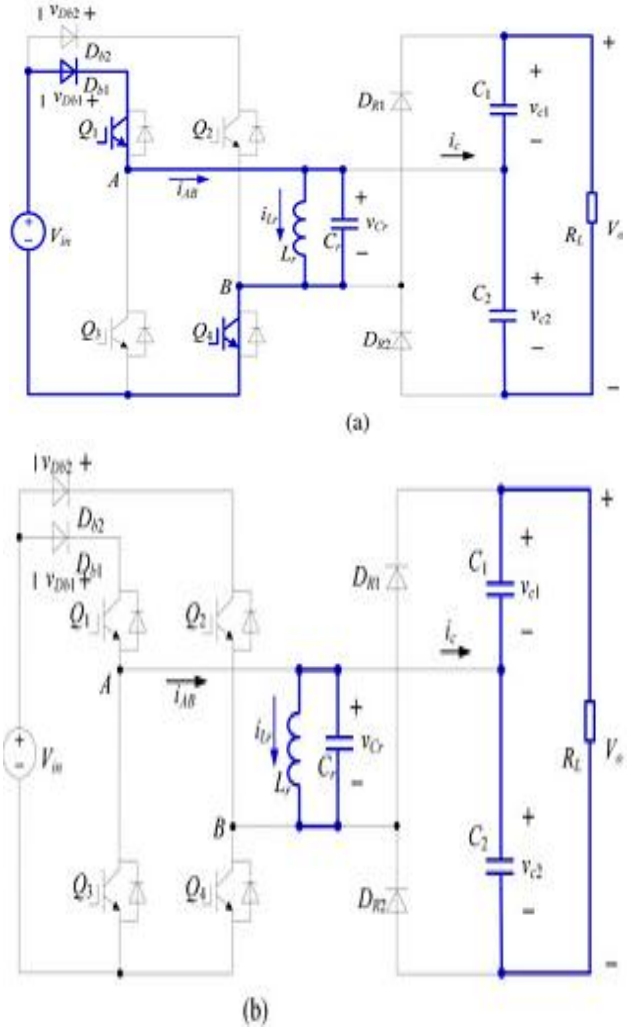

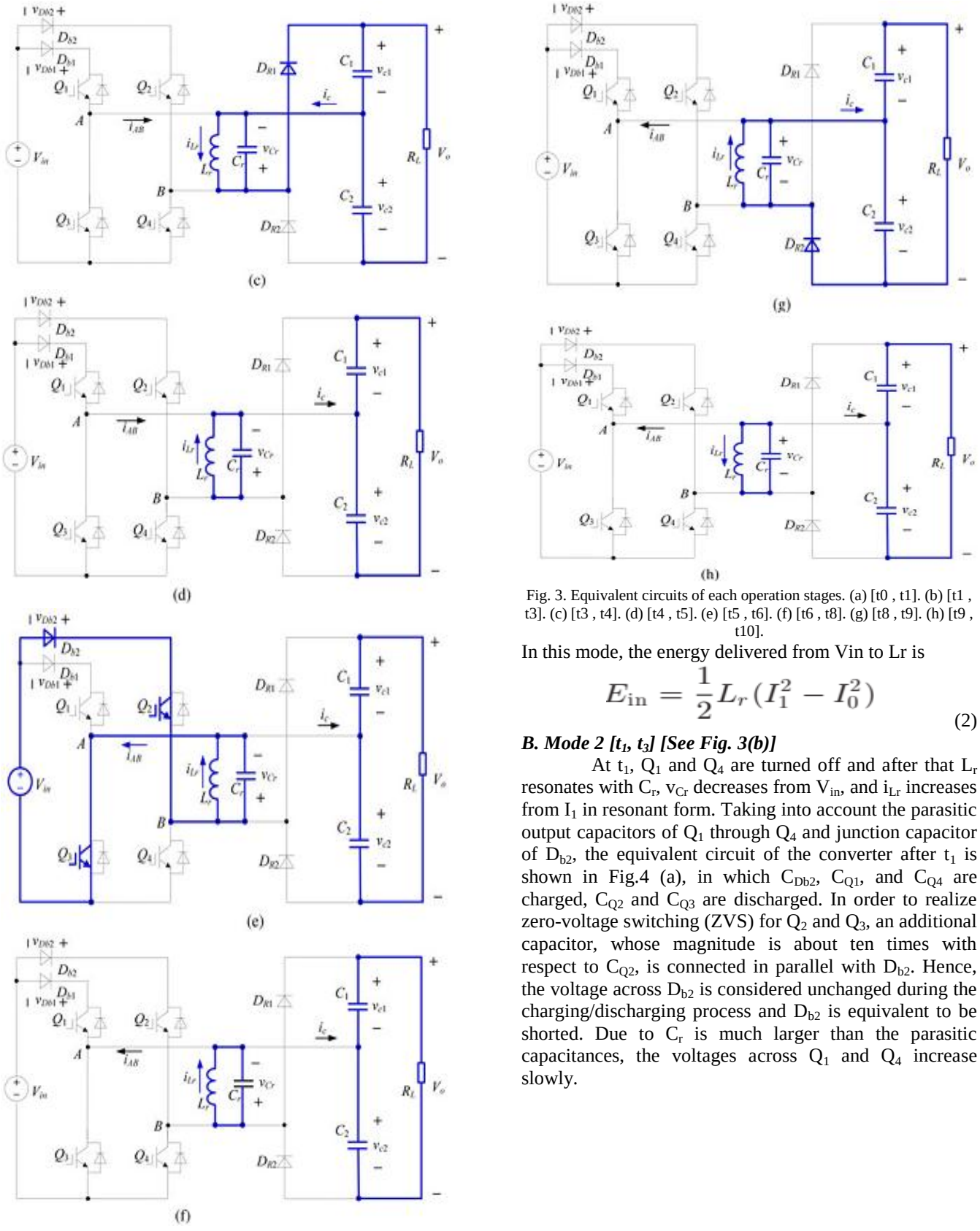

Fig. 3. Equivalent circuits of each operation stages. (a) [t0 , t1]. (b) [t1 , t3]. (c) [t3 , t4]. (d) [t4 , t5]. (e) [t5 , t6]. (f) [t6 , t8]. (g) [t8 , t9]. (h) [t9 , t10].

In this mode, the energy delivered from Vin to Lr is

$$E_{\text{in}} = \frac{1}{2} L_r (I_1^2 - I_0^2) \tag{2}$$

B. Mode 2 [t_1, t_3] [See Fig. 3(b)]

At t_1, Q_1 and Q_4 are turned off and after that L_r resonates with C_r, v_{Cr} decreases from V_{in}, and i_{Lr} increases from I_1 in resonant form. Taking into account the parasitic output capacitors of Q_1 through Q_4 and junction capacitor of D_{b2}, the equivalent circuit of the converter after t_1 is shown in Fig.4 (a), in which C_{Db2}, C_{Q1}, and C_{Q4} are charged, C_{Q2} and C_{Q3} are discharged. In order to realize zero-voltage switching (ZVS) for Q_2 and Q_3, an additional capacitor, whose magnitude is about ten times with respect to C_{Q2}, is connected in parallel with D_{b2}. Hence, the voltage across D_{b2} is considered unchanged during the charging/discharging process and D_{b2} is equivalent to be shorted. Due to C_r is much larger than the parasitic capacitances, the voltages across Q_1 and Q_4 increase slowly.

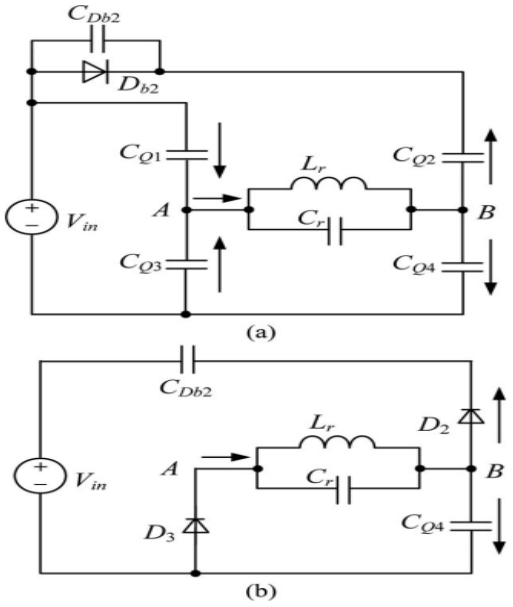

Fig. 4. Further equivalent circuits of Mode 2. (a) [t_1, t_2]. (b) [t_2, t_3].

As a result, Q_1 and Q_4 are turned off at almost zero voltage in this mode. When v_{Cr} drops to zero, i_{Lr} reaches its maximum magnitude. After that, v_{Cr} increases in negative direction and i_{Lr} declines in resonant form. At t_2, $v_{Cr} = -V_{in}$, the voltages across Q_1 and Q_4 reach V_{in}, the voltages across Q_2 and Q_3 fall to zero andthe two switches can be turned on under zero-voltage condition. It should be noted that although Q_2 and Q_3 could be turnedon after t_2, there are no currents flowing through them. After t_2, L_r continues to resonate with C_r, v_{Cr} increases in negative direction from $-V_{in}$, i_{Lr} declines in resonant form. D_{b2} willhold reversed-bias voltage and the voltage across Q_4 continuesto increase from V_{in}. The voltage across Q_1 is kept at V_{in}. Theequivalent circuit of the converter after t_2 is shown in Fig. 4(b), in which D_2 and D_3 are the antiparallel diodes of Q_2 and Q_3, respectively. This mode runs until v_{Cr} increases to $-Vo/2$ and i_{Lr} reduces to I_2, at t_3, the voltage across Q_4 reaches $Vo/2$ andthe voltage across D_{b2} reaches $Vo/2 - V_{in}$. It can be seen that during t_1 to t_3, no power is transferred fromthe input source or to the load, and the whole energy stored in the LC resonant tank is unchanged, i.e.,

$$\frac{1}{2}L_r I_1^2 + \frac{1}{2}C_r V_{\text{in}}^2 = \frac{1}{2}L_r I_2^2 + \frac{1}{2}C_r\left(\frac{V_o}{2}\right)^2 \tag{3}$$

We have

$$i_{Lr}(t) = \frac{V_{\text{in}}}{Z_r}\sin\left[\omega_r(t-t_1)\right] + I_1\cos\left[\omega_r(t-t_1)\right] \tag{4}$$

$$v_{Cr}(t) = V_{\text{in}}\cos\left[\omega_r(t-t_1)\right] - I_1 Z_r \sin\left[\omega_r(t-t_1)\right] \tag{5}$$

$$T_2 = \frac{1}{\omega_r}\left[\arcsin\left(\frac{V_{\text{in}}}{\sqrt{V_{\text{in}}^2 + \frac{L_r I_1^2}{C_r}}}\right) + \arcsin\left(\frac{V_o}{2\sqrt{V_{\text{in}}^2 + \frac{L_r I_1^2}{C_r}}}\right)\right] \tag{6}$$

Where $\omega r = 1\sqrt{L_r C_r}$, $Z_r = L_r/C_r$, and T_2 is the time interval of t_1 to t_3.

C. Mode 3 [t_3, t_4] [See Fig. 3(c)]

At t_3, $v_{Cr} = -Vo/2$, D_{R1} conducts naturally, C_1 is charged by iLr through D_{R1}, v_{Cr} keeps unchanged, and i_{Lr} decreases linearly. At t_4, $i_{Lr} = 0$. The time interval of t_3 to t_4 is

$$T_3 = \frac{2I_2 L_r}{V_o} \tag{7}$$

The energy delivered to load side in this mode is

$$E_{\text{out}} = \frac{V_o I_2 T_3}{4} \tag{8}$$

The energy consumed by the load in half-switching period is

$$E_R = \frac{V_o I_o T_s}{2} \tag{9}$$

Assuming 100% conversion efficiency of the converter andaccording to the energy conversation rule, in half-switchingperiod

$$E_{\text{in}} = E_{\text{out}} = E_{\text{R}} \tag{10}$$

Combining (7), (8), (9), and (10), we have

$$I_2 = V_o\sqrt{\frac{I_o T_s}{V_o L_r}} \tag{11}$$

$$T_3 = 2\sqrt{\frac{T_s I_o L_r}{V_o}} \tag{12}$$

D. Mode 4 [t_4, t_5] [See Fig. 3(d)]

At t_4, i_{Lr} decreases to zero and the current flowing through D_{R1} also decreases to zero, and D_{R1} is turned off with zerocurrent switching (ZCS); therefore, there is no reverse recovery. After t_4, L_r resonates with C_r, C_r is discharged through L_r, vC_r increases from $-Vo/2$ in positive direction, and i_{Lr} increases from zero in negative direction. Meanwhile, the voltage across Q_4 declines from $Vo/2$. At t_5, $v_{Cr} = -V_{in}$, and $i_{Lr} = -I_3$. In this mode, the whole energy stored in the LC resonant tank is unchanged, i.e., where T_4 is the time interval of t_4 to t_5.

$$\frac{1}{2}C_r\left(\frac{V_o}{2}\right)^2 = \frac{1}{2}L_r I_3^2 + \frac{1}{2}C_r V_{\text{in}}^2 \tag{13}$$

We have

$$I_0 = I_3 = \frac{1}{2}\sqrt{\frac{C_r(V_o^2 - 4V_{\text{in}}^2)}{L_r}} \tag{14}$$

$$i_{Lr}(t) = -\frac{V_o}{2\omega_r L_r}\sin\left[\omega_r(t-t_5)\right] \quad (15)$$

$$v_{Cr}(t) = \frac{-V_o\cos\left[\omega_r(t-t_5)\right]}{2} \quad (16)$$

$$T_4 = \frac{1}{\omega_r}\arccos\left(\frac{2V_{in}}{V_o}\right) \quad (17)$$

E. Mode 5 [t_5, t_6] [See Fig. 3(e)]

If Q_2 and Q_3 are turned on before t5, then after t_5, L_r is charged by V_{in} through Q_2 and Q_3, i_{Lr} increases in negative direction, and the mode is similar to Mode 1. If Q_2 and Q_3 are not turned on before t_5, then after t_5, L_r will resonate with C_r, the voltage of node A vA will increasefrom zero and the voltage of node B vB will decay from V_{in}; zero-voltage condition will be lost if Q_2 and Q_3 are turned onat the moment. Therefore, Q_2 and Q_3 must be turned on before t_5 to reduce switching loss. The operation modes during [t_6, t_{10}] are similar to Modes 2–4, and the detailed equivalent circuits are shown in Fig. 3(f)–(h). During [t_6, t_{10}], Q_2 and Q_3 are turned off at almost zerovoltage, Q_1 and Q_4 are turned on with ZVS, and D_{R2} is turned off with ZCS.

III. INDUCTION MOTOR

An asynchronous motor type of an induction motor is an AC electric motor in which the electric current in the rotor needed to produce torque is obtained by electromagnetic induction from the magnetic field of the stator winding. An induction motor can therefore be made without electrical connections to the rotor as are found in universal, DC and synchronous motors. An asynchronous motor's rotor can be either wound type or squirrel-cage type.

Three-phase squirrel-cage asynchronous motors are widely used in industrial drives because they are rugged, reliable and economical. Single-phase induction motors are used extensively for smaller loads, such as household appliances like fans.

Although traditionally used in fixed-speed service, induction motors are increasingly being used with variable-frequency drives (VFDs) in variable-speed service. VFDs offer especially important energy savings opportunities for existing and prospective induction motors in variable-torque centrifugal fan, pump and compressor load applications. Squirrel cage induction motors are very widely used in both fixed-speed and variable-frequency drive (VFD) applications. Variable voltage and variable frequency drives are also used in variable-speed service.

In both induction and synchronous motors, the AC power supplied to the motor's stator creates a magnetic field that rotates in time with the AC oscillations. Whereas a synchronous motor's rotor turns at the same rate as the stator field, an induction motor's rotor rotates at a slower speed than the stator field. The induction motor stator's magnetic field is therefore changing or rotating relative to the rotor. This induces an opposing current in the induction motor's rotor, in effect the motor's secondary winding, when the latter is short-circuited or closed through external impedance. The rotating magnetic flux induces currents in the windings of the rotor; in a manner similar to currents induced in a transformer's secondary winding(s). The currents in the rotor windings in turn create magnetic fields in the rotor that react against the stator field. Due to Lenz's Law, the direction of the magnetic field created will be such as to oppose the change in current through the rotor windings. The cause of induced current in the rotor windings is the rotating stator magnetic field, so to oppose the change in rotor-winding currents the rotor will start to rotate in the direction of the rotating stator magnetic field. The rotor accelerates until the magnitude of induced rotor current and torque balances the applied load. Since rotation at synchronous speed would result in no induced rotor current, an induction motor always operates slower than synchronous speed. The difference, or "slip," between actual and synchronous speed varies from about 0.5 to 5.0% for standard Design B torque curve induction motors.

The induction machine's essential character is that it is created solely by induction instead of being separately excited as in synchronous or DC machines or being self-magnetized as in permanent magnet motors.

For rotor currents to be induced the speed of the physical rotor must be lower than that of the stator's rotating magnetic field (n_s); otherwise the magnetic field would not be moving relative to the rotor conductors and no currents would be induced. As the speed of the rotor drops below synchronous speed, the rotation rate of the magnetic field in the rotor increases, inducing more current in the windings and creating more torque. The ratio between the rotation rate of the magnetic field induced in the rotor and the rotation rate of the stator's rotating field is called slip. Under load, the speed drops and the slip increases enough to create sufficient torque to turn the load. For this reason, induction motors are sometimes referred to as asynchronous motors. An induction motor can be used as an induction generator, or it can be unrolled to form a linear induction motor which can directly generate linear motion.

Synchronous Speed:

The rotational speed of the rotating magnetic field is called as synchronous speed.

$$Ns = \frac{120 \text{ x } f}{P} \quad (RPM) \quad (18)$$

Where, f = frequency of the supply

P = number of poles

Slip:

Rotor tries to catch up the synchronous speed of the stator field, and hence it rotates. But in practice, rotor never succeeds in catching up. If rotor catches up the stator speed, there won't be any relative speed between the stator flux and the rotor, hence no induced rotor current and no torque production to maintain the rotation. However, this won't stop the motor, the rotor will slow down due to lost of torque, and the torque will again be exerted due to relative speed. That is why the rotor rotates at speed which is always less the synchronous speed.
The difference between the synchronous speed (Ns) and actual speed (N) of the rotor is called as slip.

$$\% \text{ slip} \quad s = \frac{Ns - N}{Ns} \times 100 \qquad (19)$$

III.MATLAB/SIMULATION RESULTS

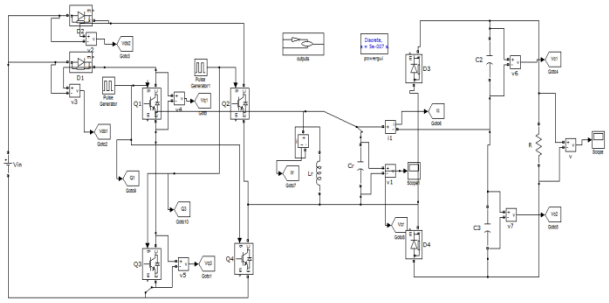

Fig.5 Simulink model of the proposed resonant step-up converter

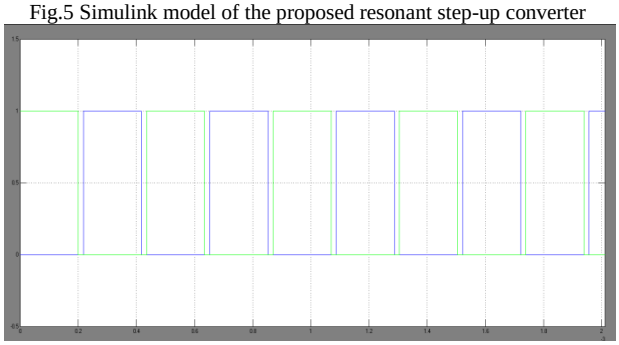

Q_1, Q_3

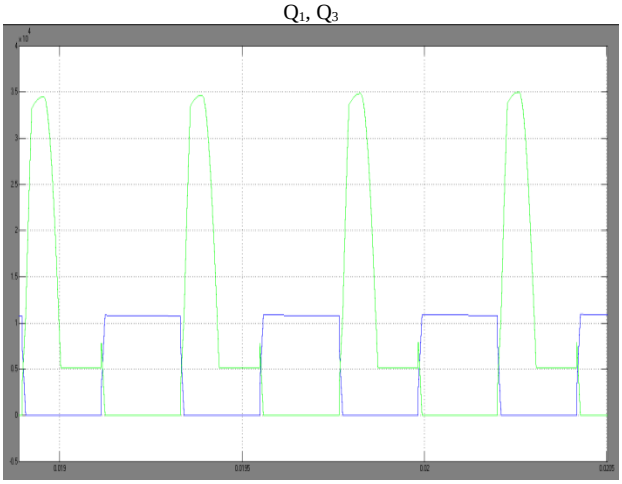

V_{q1}, V_{q3}

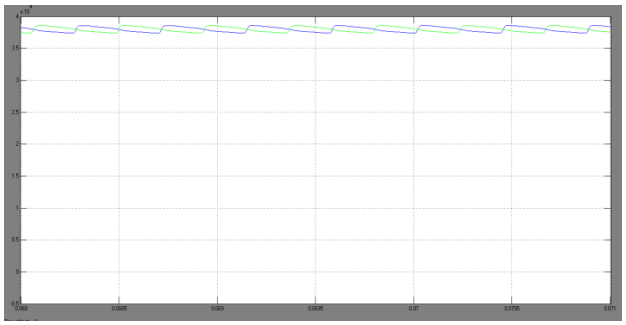

V_{c1}, V_{c2}

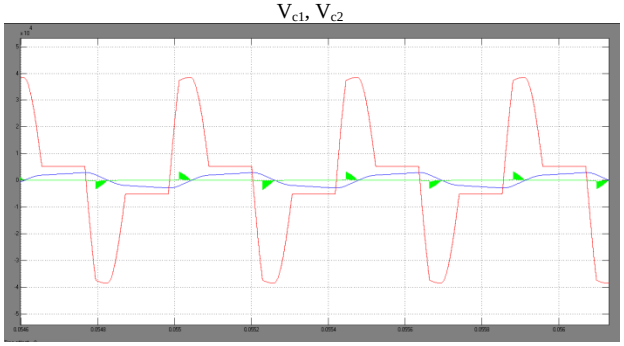

I_{Lr}, I_c, V_{cr}

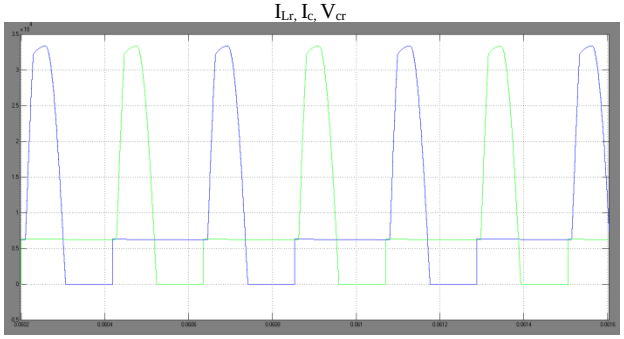

V_{db1}, V_{db2}

(a)

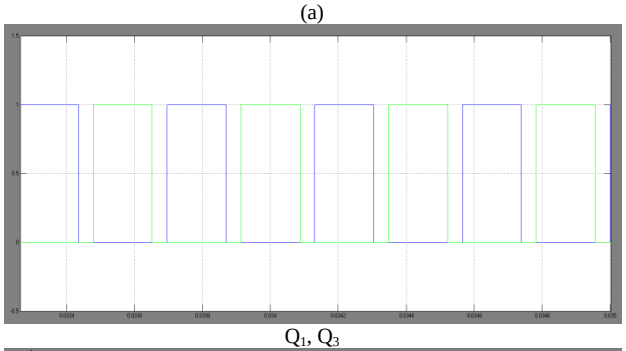

Q_1, Q_3

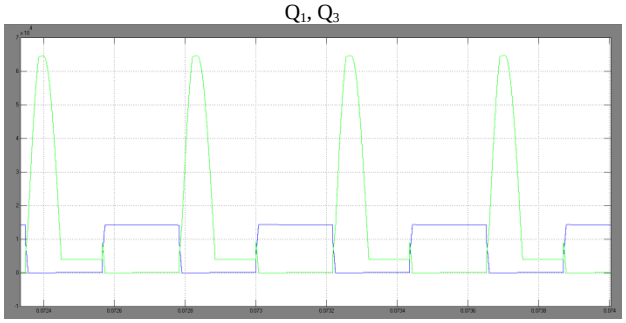

V_{q1}, V_{q3}

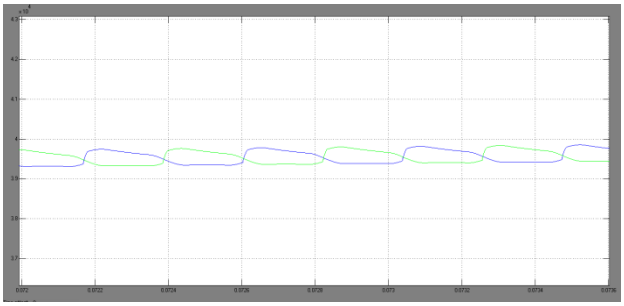

V_{c1}, V_{c2}

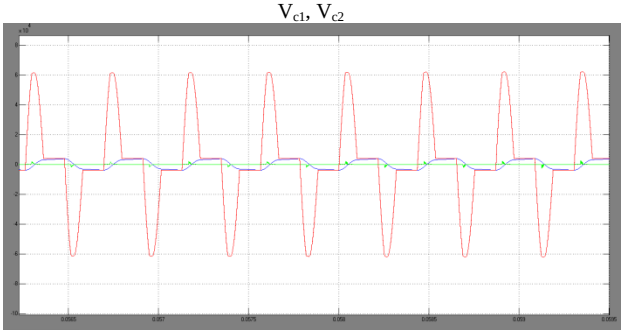

I_{Lr}, I_c, V_{cr}

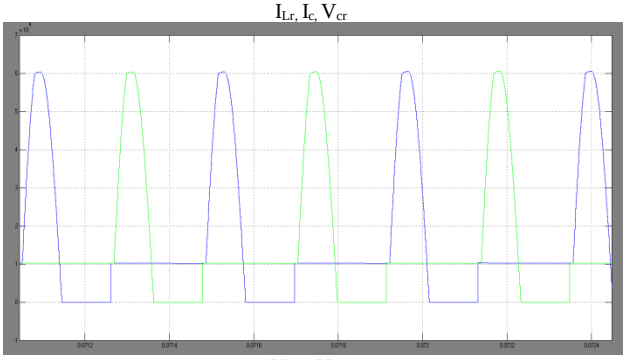

V_{db1}, V_{db2}

(b)

Fig.6. Steady-state simulation results under different load conditions when V_{in} = 4kV. (a) 5 MW. (b) 1 MW.

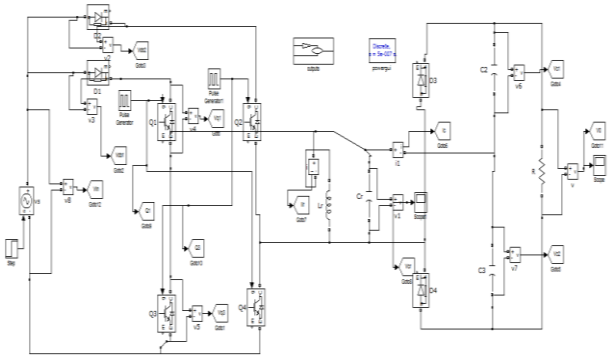

Fig.7 Simulink model of the proposed resonant step-up converter under voltage and load current step condition

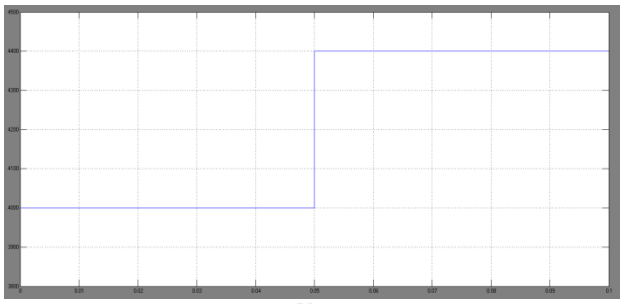

V_{in}

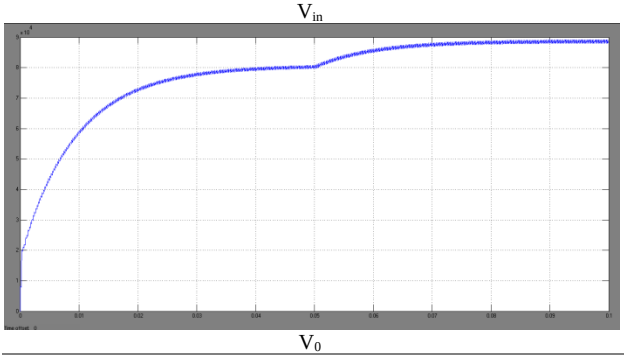

V_0

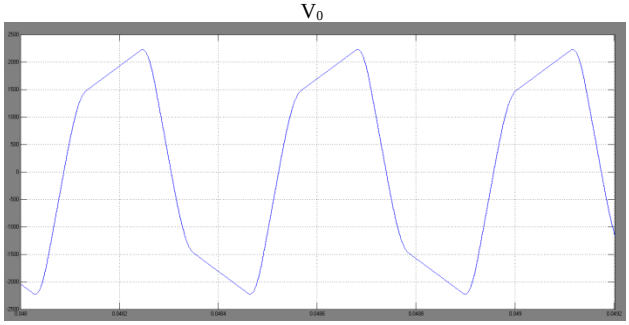

I_{Lr}

(a)

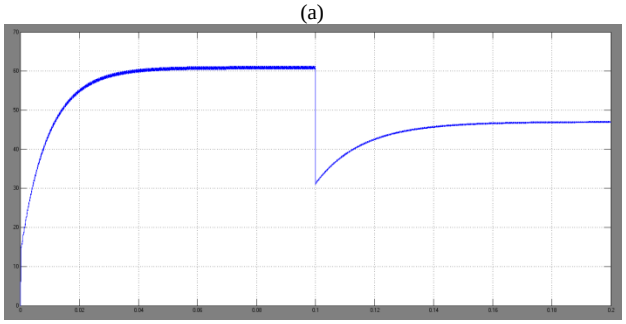

I_0

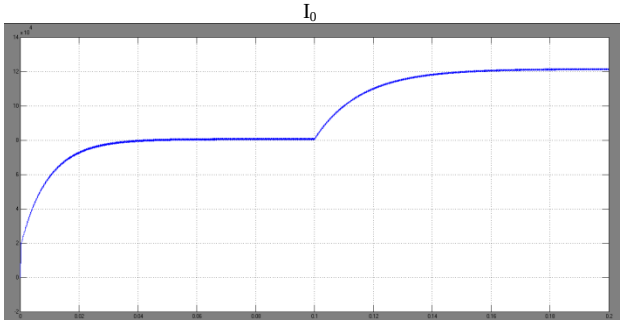

V_0

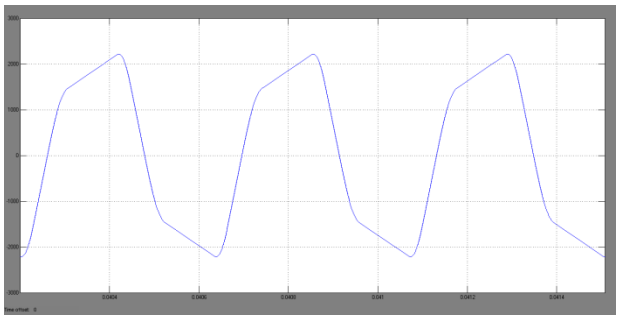

I_{Lr}

(b)

Fig.8. Dynamic simulation results. (a) Input voltage step. (b) Load step.

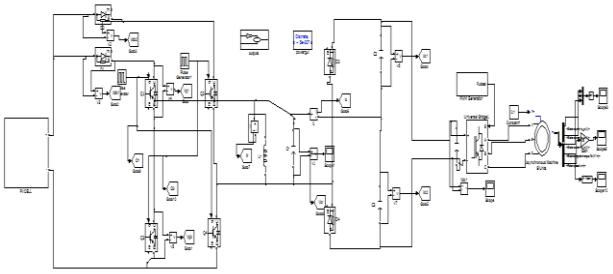

Fig.9 Simulink model of the PV connected resonant step-up converter with induction motor drive applications.

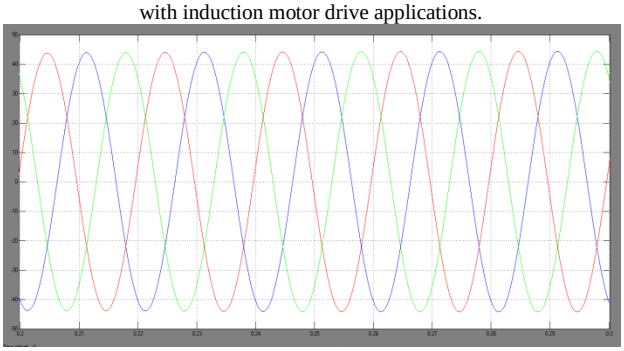

Fig.10 Stator Current of induction motor

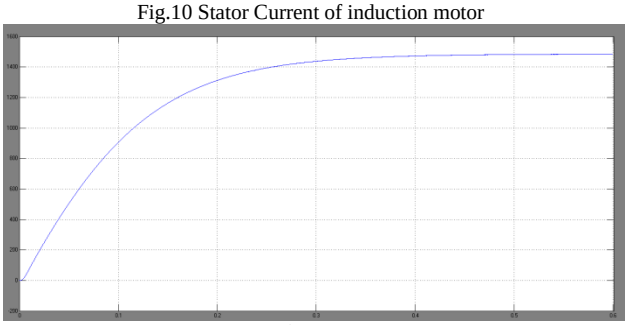

Fig.11 Speed of the induction motor

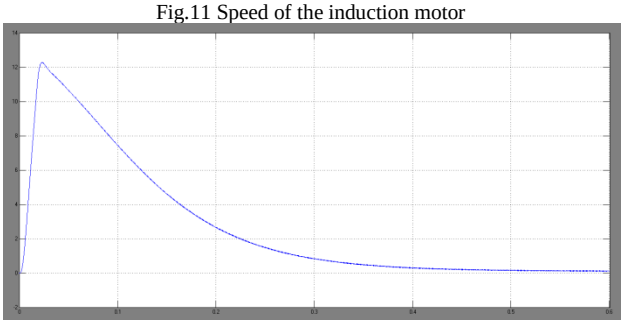

Fig.12 Torque characteristics of the induction motor

IV.CONCLUSIONS

A novel resonant dc–dc converter is proposed in this paper, which can achieve very high step-up voltage gain and it is suitable for high-power high-voltage applications. The converter utilizes the resonant inductor to deliver power by charging from the input and discharging at the output. The resonant capacitor is employed to achieve zero-voltage turn-on and turn-off for the active switches and ZCS for the rectifier diodes.In this paper, the converter was designed to drive a three phase induction motor directly from PV solar energy and was conceived to be a commercially viable high efficiency, and high robustness.

REFERENCES

[1].Wu Chen, Member, IEEE, Xiaogang Wu, Liangzhong Yao, Senior Member, IEEE, Wei Jiang, Member, IEEE, and Renjie Hu"A Step-up Resonant Converter for Grid-Connected Renewable Energy Sources"IEEE Transactions On Power Electronics, Vol. 30, No. 6, June 2015.

[2] CIGRE B4-52 Working Group, HVDC Grid Feasibility Study. Melbourne, Vic., Australia: Int. Council Large Electr. Syst., 2011.

[3] A. S. Abdel-Khalik, A. M. Massoud, A. A. Elserougi, and S. Ahmed, "Optimum power transmission-based droop control design for multi-terminal HVDC of offshore wind farms," IEEE Trans. Power Syst., vol. 28, no. 3, pp. 3401–3409, Aug. 2013.

[4] F. Deng and Z. Chen, "Design of protective inductors for HVDC transmission line within DC grid offshore wind farms," IEEE Trans. Power Del., vol. 28, no. 1, pp. 75–83, Jan. 2013.

[5] F. Deng and Z. Chen, "Operation and control of a DC-grid offshore wind farm under DC transmission system faults," IEEE Trans. Power Del., vol. 28, no. 1, pp. 1356–1363, Jul. 2013.

[6] C. Meyer, "Key components for future offshore DC grids," Ph.D. dissertation, RWTH Aachen Univ., Aachen, Germany, pp. 9–12, 2007.

[7] W. Chen, A. Huang, S. Lukic, J. Svensson, J. Li, and Z. Wang, "A comparison of medium voltage high power DC/DC converters with high step-up conversion ratio for offshore wind energy systems," in Proc. IEEE Energy Convers. Congr. Expo., 2011, pp. 584–589.

[8] L. Max, "Design and control of a DC collection grid for a wind farm," Ph.D. dissertation, Chalmers Univ. Technol., Goteborg, Sweden, pp. 15– ¨30, 2009.

[9] Y. Zhou, D. Macpherson, W. Blewitt, and D. Jovcic, "Comparison of DCDC converter topologies for offshore wind-farm application," in Proc. Int. Conf. Power Electron. Mach. Drives, 2012, pp. 1–6.

[10] S. Fan, W. Ma, T. C. Lim, and B. W. Williams, "Design and control of a wind energy conversion system based on a resonant dc/dc converter," IET Renew. Power Gener., vol. 7, no. 3, pp. 265–274, 2013.

[11] F. Deng and Z. Chen, "Control of improved full-bridge three-level DC/DC converter for wind turbines in a DC grid," IEEE Trans. Power Electron., vol. 28, no. 1, pp. 314–324, Jan. 2013.

[12] C. Meyer, M. Hoing, A. Peterson, and R. W. De Doncker, "Control and ¨ design of DC grids for offshore wind farms," IEEE Trans. Ind. Appl., vol. 43, no. 6, pp. 1475–1482, Nov./Dec. 2007.

[13] C. Meyer and R. W. De Doncker, "Design of a three-phase series resonant converter for offshore DC grids," in Proc. IEEE Ind. Appl. Soc. Conf., 2007, pp. 216–223.